Deep–Sea Research I 203 (2024) 104224

Contents lists available at ScienceDirect

Deep-Sea Research Part I

journal homepage: www.elsevier.com/locate/dsri

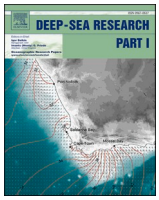

Controls on long-term changes in bathyal bivalve biomass: The Pleistocene glacial–interglacial record in the eastern Mediterranean

Antonia Porz [a], Martin Zuschin [a], Luke Strotz [a,b], Efterpi Koskeridou [c], Kobe Simoens [d], Renata Lukić [e], Danae Thivaiou [c], Frédéric Quillévéré [f], Konstantina Agiadi [a,*]

[a] University of Vienna, Department of Palaeontology, Josef-Holaubek-Platz 2, UZA II, 1090, Vienna, Austria
[b] State Key Laboratory of Continental Dynamics, Shaanxi Key Laboratory of Early Life & Environments and Department of Geology, Northwest University, Xi'an, 710069, China
[c] Department of Historical Geology and Paleontology, National and Kapodistrian University of Athens, Panepistimioupolis, 15784, Athens, Greece
[d] IMBRSea Program, Ghent University - Marine Biology Research Group, Krijgslaan 281/S8 - 9000, Ghent, Belgium
[e] Department of Geology, University of Zagreb, Horvatovac 102a, 10000, Zagreb, Croatia
[f] Université Claude Bernard Lyon 1, ENS de Lyon, CNRS, UMR 5276 LGL-TPE, F-69622, Villeurbanne, France

ARTICLE INFO

Keywords:
Temperature–size rule
Shells
Molluscs
Quaternary
Climate change
Greece

ABSTRACT

The biomass of aquatic organisms largely determines the mass and energy flow within an ecosystem, but the long-term impact of environmental change on biomass is not well constrained for a number of clades. Here, we test the hypothesis that bivalve biomass is negatively impacted by warming climate over time. This study is based on a fossil marine bivalve fauna recovered from hemipelagic sediments deposited in the eastern Mediterranean during climate cycles (marine isotope stages (MIS) 22–18; 900–712 kyr B.P.) of the Early–Middle Pleistocene Transition. We reconstruct individual shell biomasses from fossils and discuss the various biotic and abiotic factors that controlled long-term shell biomass patterns across this important interval in the Earth climate system. The results are contrary to the original hypothesis, suggesting that the response to temperature is not universal. Nevertheless, a decrease in median biomass is observed during the MIS 19 warm period and can be possibly attributed to the combined effect of multiple drivers that cooperated at that critical time in the past, including higher temperature and primary productivity, reduced ventilation of the sea floor, biodiversity changes due to geographic range shifts, and considering species- and age-specific thermal tolerances. Generally, bivalve biomass at the community level is determined by relative abundance and shell biomass-frequency distribution. In our study, the relative abundance and median biomass of small species do not increase or decrease, respectively, in warmer periods. However, larger species are negatively affected by warming both in terms of relative abundance and biomass.

1. Introduction

Climate change impacts both the size and metabolism of marine organisms (Daufresne et al., 2009; Ohlberger, 2013), which in turn influences the structure and functioning of marine ecosystems (Hildrew et al., 2007). Biomass is directly correlated with trophic level (Estes et al., 2011), meaning that individual-as well as community-level changes in biomass can have cascading effects on the entire food web. According to the temperature–size rule for ectotherms (Atkinson, 1994), with increasing ambient water temperature, individuals grow faster during their early life stage, reaching maturity at smaller individual biomasses and thereby forming a population with smaller individuals. Higher temperatures also expedite biochemical reactions and increase the availability of organic matter and energy. These can induce faster growth and potentially lead to smaller sizes (Ohlberger, 2013). On the other hand, at least at large scales, higher temperatures may lead to niche expansion through the inclusion of larger size classes (Bryant and McClain, 2022). In addition, ocean warming results in deoxygenation and acidification, which prevent organisms from growing to large sizes (Gobler et al., 2014; Watson et al., 2012). However, adaptation strategies (Atkinson, 1995; Audzijonyte et al., 2020) are also impacting the biomass patterns at species and community levels. Moreover, species-specific thermal range limits determine the ability of a species to cope with changing thermal conditions. It is assumed that the greater

* Corresponding author.
E-mail address: konstantina.agiadi@univie.ac.at (K. Agiadi).

https://doi.org/10.1016/j.dsr.2023.104224
Received 29 July 2023; Received in revised form 30 November 2023; Accepted 21 December 2023
Available online 27 December 2023

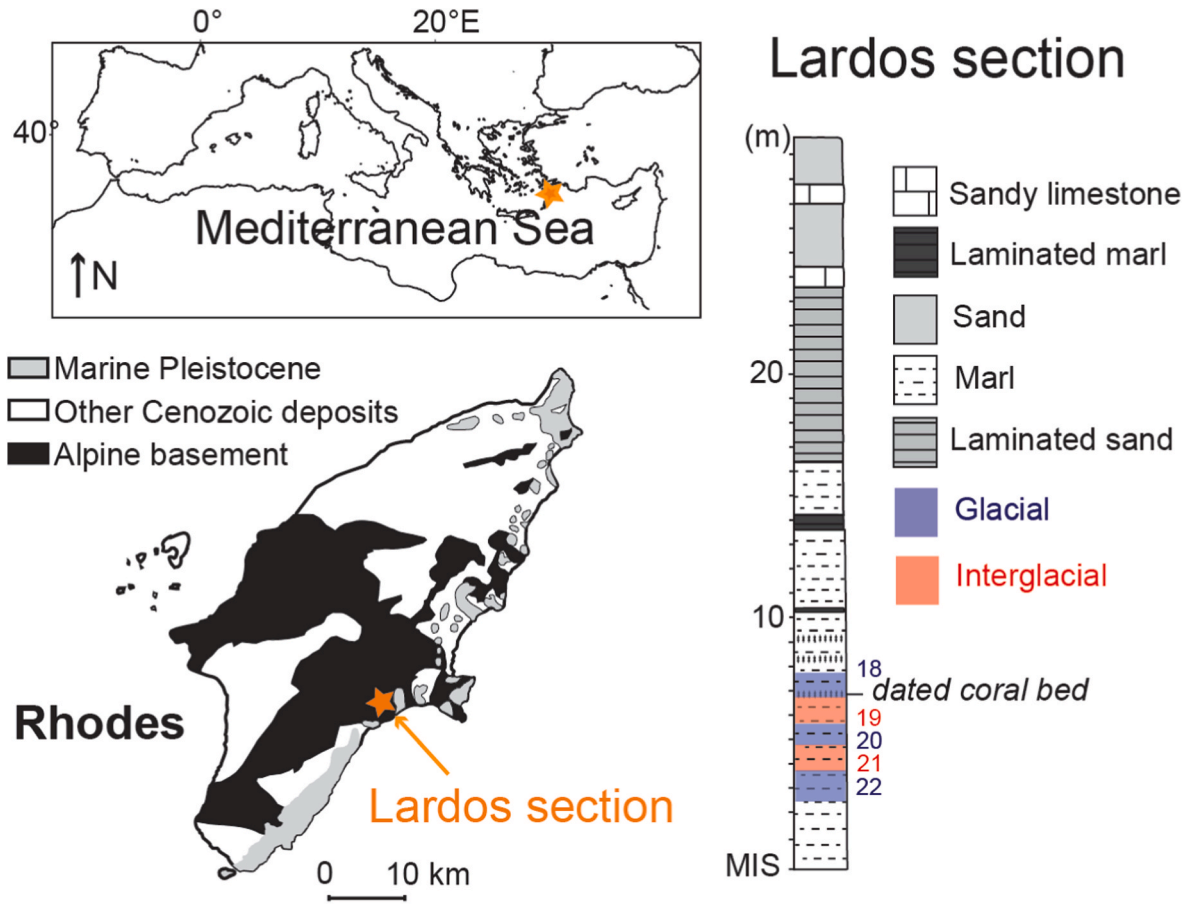

Fig. 1. Location of the island of Rhodes in the Mediterranean Sea indicating the study area and the stratigraphic column of the Lardos section. MIS: marine isotope stage. Modified after Agiadi et al. (2023).

temperature fluctuations in temperate latitudes result in wider physiological tolerance windows for poikilothermic animals that inhabit these environments, while the smaller temperature fluctuations in tropical latitudes lead to narrower tolerance windows (Dobzhansky, 1950; Stevens, 1989).

Despite its clear significance, evaluating and predicting the long-term effects of climate change on the size structure of modern marine assemblages is challenging, because these effects are difficult to disentangle from the impacts of other anthropogenic stressors, such as habitat deterioration and overexploitation. Using the fossil record, it is possible to track biotic responses to natural climate variability on much longer timescales and during periods of more extreme paleoclimatic perturbations than is possible with ecological monitoring of modern systems (Dietl et al., 2015). The Early–Middle Pleistocene Transition (EMPT), in particular, was a critical time in Earth history, when climate patterns shifted from a 40-kyr cycle to stronger, 100-kyr glacial–interglacial cycles including millennial-scale variability (Hodell et al., 2023; Hodell and Channell, 2016), with concomitant growth of the Northern Hemisphere ice-sheets (Lisiecki and Raymo, 2005; McClymont et al., 2013). During the transition from glacial marine isotope stage (MIS) 20 to the warmer part of MIS 19 (interstadial MIS 19c), in particular, sea surface temperature shifted by more than 4 °C within a few thousand years (McClymont et al., 2013; PAGES, 2016; Rodrigues et al., 2017) and the recorded shift in the Mediterranean Sea was around 4 °C (Konijnendijk et al., 2015; Marino et al., 2020a; Quivelli et al., 2021). Although the rate of change is more than one order of magnitude slower than modern climate change, the magnitude of the temperature increase is in line with the IPCC-predicted mean surface temperature increase until the end of the 21st century under the high greenhouse gas (GHG) emissions scenario (IPCC et al., 2021; 2019; Lotze et al., 2019). Moreover, due to similar astronomical configuration of orbital parameters, interstadial MIS 19c is considered an exceptional analogue to the Holocene interglacial (Marino et al., 2020b, 2015; PAGES, 2016; Regattieri et al., 2019; Tzedakis, 2010). Thus, understanding the impact of increasing sea surface temperatures on Early–Middle Pleistocene faunas has implications for understanding the limitations of natural systems and quantifying how current climate warming will disrupt the structure of modern marine communities in the Mediterranean. Indeed, previous studies demonstrated that even deep-sea organisms from around the world have been affected directly or indirectly (e.g., due to sea-level changes) by Pleistocene climate alternations (Agiadi et al., 2018, 2023; Girone et al., 2023; Huang et al., 2019; Lin et al., 2023; Melo et al., 2022; Peral et al., 2020; Urra et al., 2023; Yasuhara and Cronin, 2008). Furthermore, in the Mediterranean, the sea-level changes resulting from Pleistocene climate cycles changed the Gibraltar sill depth, which has been suspected to have affected thermohaline circulation thereby distorting the temperature gradient and impacting marine fauna (Agiadi et al., 2011; La Perna, 2003).

Suspension-feeding bivalves filter organic and inorganic matter from the water column (Bonsdorff and Blomqvist, 1993; Gili and Coma, 1998), linking the pelagic to the benthic ecosystems. Changes in their biomass and abundance can therefore lead to shifts in the pelagic food-web structure and influence multiple trophic levels (Karlson et al., 2021). In deep time, biomass changes in marine bivalves have been documented after major environmental crises and associated to changes in the oxygenation of the seafloor, oceanic circulation strength and primary productivity (Caswell and Coe, 2013; Foster et al., 2020; Huang et al., 2023; Mukhopadhyay et al., 2023; Rhodes and Thayer, 1991; Twitchett, 2007), which are all affected by seawater temperature (Piazza et al., 2020). Apart from biomass changes due to the impact of

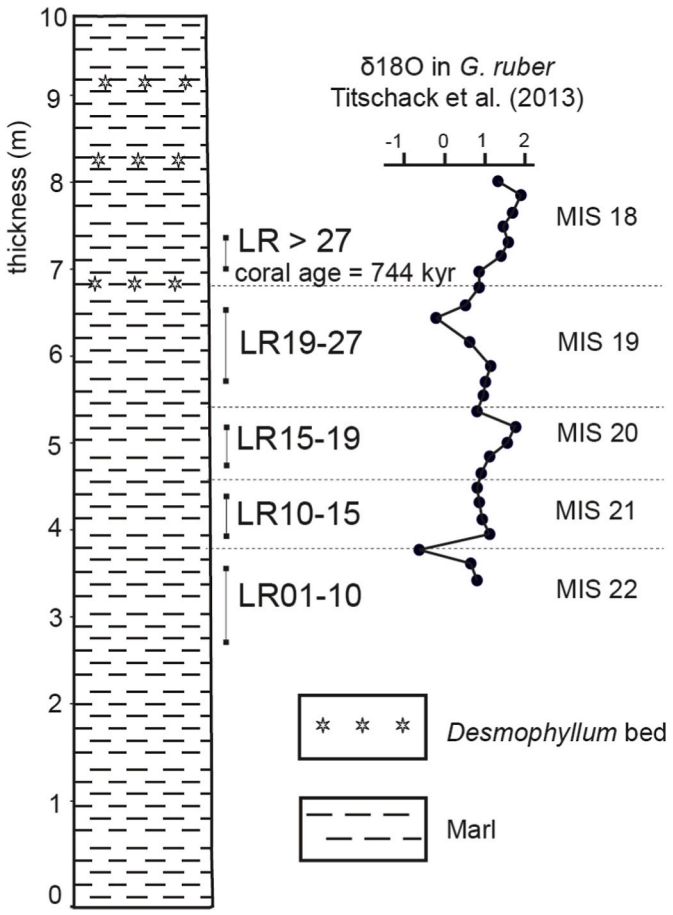

Fig. 2. Detail of the lithostratigraphic column indicating the sampled intervals, and planktonic foraminiferal (*Globigerinoides ruber*) stable isotope ($(\delta^{18}O_{VPDB})$) stratigraphic record of the Lardos section (Titschack et al., 2013).

temperature on bivalve physiology, the relative abundance of large bivalves has been found to increase with higher temperature as they expand their distribution range more easily, as for example in the Northeast Pacific continental shelf during the Pleistocene (Roy et al., 2001).

In this study, we test the hypothesis of a negative correlation between climate warming and biomass for bathyal bivalves, by assessing the size structure of their assemblages in the Eastern Mediterranean during climate cycles of the EMPT corresponding to MIS 22 to MIS 18 (900–712 kyr B.P.; (Lisiecki and Raymo, 2005). We use fossil bivalve shells collected from chronostratigraphically well-constrained upper bathyal deposits of the Lindos Bay Formation on the island of Rhodes, southeast Aegean Sea, and we estimate shell dimensions (Novack-Gottshall, 2008) and bivalve biomass from biovolume (Powell and Stanton, 1985).

2. Material and methods

2.1. Sampling and processing

The material used in this study originates from the Lindos Bay Formation exposed at Lardos, Rhodes, Greece (Fig. 1). On Rhodes, the Mesozoic–Paleogene limestone substratum is overlain by marine siliciclastic-carbonate Pleistocene deposits. Since the Pliocene, the compressive regime of this area of the Hellenic fore-arc and the concomitant opening of the >4000 m deep Rhodes Basin have triggered rapid vertical tectonic motions that resulted in the deposition and then uplift of Pleistocene marine sediments that are now exposed along the eastern coast of the island (Fig. 1) (Cornée et al., 2006, 2019; Van Hinsbergen et al., 2007). The Early–Middle Pleistocene hemipelagic sediments of the Lindos Bay Formation sampled for this study were deposited at bathyal depths during the maximum flooding of this tectonically driven transgression-regression cycle (Cornée et al., 2019; Milker et al., 2017; Quillévéré et al., 2019). This occurrence of Pleistocene deep-water sediments accessible on land is unique for the eastern Mediterranean, providing a valuable reference point for studying the Early–Middle Pleistocene marine faunas of the region (Quillévéré et al., 2016).

The studied section is located near the village of Lardos on southeastern Rhodes (36°05′19.5″N 28°00′35.9″E). It comprises 30 m of marine marls and sands corresponding to the upper part of the Lindos Bay Formation and the lower part of the Cape Arkhangelos Formation, respectively (Titschack et al., 2013). Five marly intervals of the Lindos Bay Formation were sampled from the lower part of the section and they correspond to the marine isotope stages MIS 22 to MIS 18 (Fig. 2), as determined by correlating the sampled levels with the chronostratigraphic framework previously established for this section by Titschack et al. (2013). The samples were taken so as to be centered in each MIS interval (Fig. 2). Corroboration was further provided by U^{234}/U^{238} dating a deep-water *Desmophyllum pertusum* coral fragment collected in the section (Fig. 1), which yielded a mean age of 744 kyr (range = 616–947 kyr) (Agiadi et al., 2023). We acknowledge that MIS 21 and MIS 19 comprise several sub-stages, not all fully corresponding to interglacial conditions. For example, within MIS 19, only MIS 19c reached interglacial conditions comparable to those of the Holocene (McClymont et al., 2013; PAGES, 2016). However, the quantity of sediment material required for the present analysis was too large to allow distinguishing these sub-stages, considering the sedimentation rate estimated at 1.9 cm/kyr in the lower part of the section (Titschack et al., 2013),. Consequently, our samples are assigned to the entire MIS,

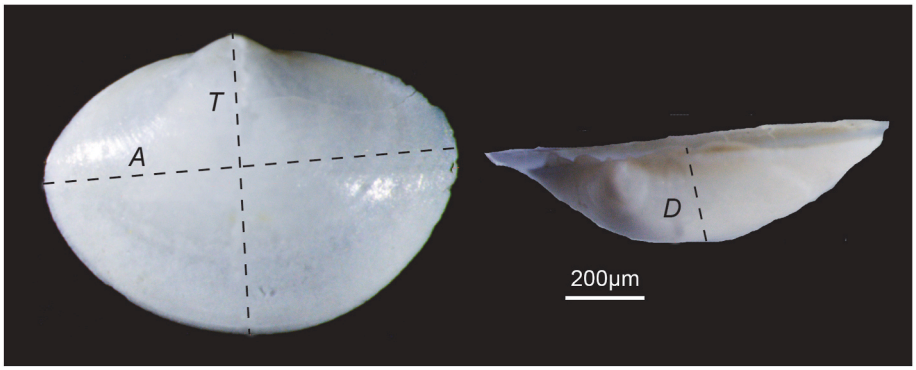

Fig. 3. *Yoldiella curta* valve (specimen LR15_19_1765) and the obtained measurements: antero-posterior length (A), transverse width (T), and dorso-ventral depth (D).

Table 1
Ecological information for the taxa identified in the bivalve assemblages of Lardos MIS 22–18: lifestyle and distributions in modern oceans by climatic zone and known depth range (from Danise and Dominici, 2023; Dominici and Danise, 2023; La Perna, 2007, 2003; Palomares and Pauly, 2022; and additional references provided for some species).

Species	Family	Climatic zone	Depth range (m)	Lifestyle	Additional References
Acar clathrata	Arcidae	Subtropical	35–70	Epifaunal	Delongueville et al. (2019)
Asperarca nodulosa	Arcidae	Subtropical	550–700	Epifaunal	
Bathyarca pectunculoides	Arcidae	Temperate	9–3330	Infaunal	
Bathyarca philippiana	Arcidae	Subtropical	125–200	Epifaunal	
Bathyspinula excisa	Bathyspinulidae	Subtropical	200–1000	Infaunal	Ceregato et al. (2007) La Perna (2003) Tabanelli (2008)
Cyclopecten hoskynsi	Propeamussiidae	Temperate	82–2064	Epifaunal	
Delectopecten vitreus	Pectinidae	Subtropical	27–4312	Epifaunal	
Ennucula corbuloides	Nuculidae	Subtropical	500–2000	Infaunal	
Kelliella miliaris	Kelliellidae	Temperate	10–1170	Infaunal	
Limatula gwyni	Limidae	Temperate	20–57	Infaunal	
Limatula subauriculata	Limidae	Temperate	110–2321	Infaunal	
Limea crassa	Limidae	Temperate	285–555	Epifaunal	
Limopsis aurita	Limopsidae	Temperate	55–1965	Epifaunal	
Microgloma sp.	Pristiglomidae	Subtropical	>500	Epifaunal/Shallow Infaunal	
Limea crassa	Limidae	Temperate	285–555	Epifaunal (motile)	
Pseudoneilonella pusio	Neilonellidae	Subtropical	>1000	Shallow Infaunal	Dominici and Danise (2023) La Perna (2003, 2007)
Yoldia minima	Yoldiidae	Subtropical	>1000	Infaunal	
Yoldiella curta	Yoldiidae	Subtropical	150–500	Infaunal	
Yoldiella lucida	Yoldiidae	Temperate	38–1000	Infaunal	
Yoldiella micrometrica	Yoldiidae	Subtropical	500–2000	Infaunal	
Yoldiella philippiana	Yoldiidae	Subtropical	150–1000	Infaunal	
Yoldiella striolata	Yoldiidae	Subtropical	>1000	Infaunal	

including both cooler and warmer sub-stages, and the results we obtain correspond therefore to a mean cold and mean warm situation in the eastern Mediterranean. Paleodepths have been estimated at 200–250 m for MIS 22–19 and at 150–200 m for MIS 18 (Agiadi et al., 2018). Sedimentation may therefore have occurred above the oxygen-minimum zone and may have been affected by wind and (internal) wave mixing (Rohling et al., 2015).

The sediment samples were weighed and wet-sieved through a 250-μm mesh. Their weights were: 1.63 kg for LR01-10, 3.33 kg for LR10-15, 2.7 kg for LR15-19, 4.73 kg for LR19-27 and 3.26 kg for LR > 27. Bivalve specimens were picked from the residues, sorted based on their morphological characteristics and identified to species level under the binocular microscope. The preservation state of the shells was noted paying particular attention to the level of fragmentation, as well as the presence of any marks of predation and/or dissolution. The number of individual species in each of the five MIS was determined in order to establish their relative abundance.

2.2. Shell biovolume and biomass estimation

For the reconstruction of shell biomass, we retained shells based on two criteria: specimens preserving enough of the hinge line to allow identification; and specimens where at least two of the three dimensions (length, width, depth) could be measured (Fig. 3). Both criteria were needed for a specimen to be included in our dataset. Following Novack-Gottshall (2008), we measured the antero-posterior length (*A*), transverse width (*T*), and dorso-ventral depth (*D*) (Fig. 3) in order to estimate the maximum body volume of our specimens, where *T* is the distance from the umbo, which is the highest part of the valve in the dorsal margin, to the ventral end of the shell; *A* is the dimension perpendicular to *T*, from the anterior to the posterior end of the shell; and *D* is the maximum thickness of the valve that is perpendicular to both *A* and *T*. Based on this *ATD* model, biovolume is: $V = 0{,}5444\ (ATD)^{0{,}896}$ and expressed in mm^3.

Next, with this biovolume estimate, we calculated the maximum biomass (in g) of each fossil specimen using the equation of Powell and Stanton (1985): $logB = (0.9576 \pm 0.0004) logV + (-4.8939 \pm 0.0065)$. This approach allows specimens of different species to be compared, because the calculated individual biomass is independent from the shape of the bivalve.

2.3. Ecological data for the identified taxa

For the taxa identified in our assemblages, we collected data on their distributions by depth and by climatic zone from SeaLifeBase (Palomares and Pauly, 2022) and from the literature (e.g. (Danise and Dominici, 2023; Dominici and Danise, 2023; La Perna, 2007, 2003) (Table 1). Specifically, *Acar clathrata* (Defiance, 1816) is distributed today in the Atlantic Ocean, between Galicia and Cabo Verde, and in the Azores archipelago at 35–40 m depth and in the Mediterranean Sea up to 70 m depth (Delongueville et al., 2019). *Bathyspinula excisa* (Philippi, 1844) was commonly found at bathyal (>200 m) depths in the Pliocene–Early Pleistocene Mediterranean (Ceregato et al., 2007; La Perna, 2003; Tabanelli, 2008), and therefore we assigned it to the subtropical zone. Although the functional traits of the identified extant species may have changed over geological time, we assumed their relative stability from the Middle Pleistocene compared to the present.

Many of the identified species live below the thermocline (Table 1) (Houpert et al., 2015). Thus, they would not be expected to have experienced large temperature variations (Melo et al., 2022; Nomade et al., 2019; Scarponi et al., 2022; Urra et al., 2023). Here, we investigated shifts in median biomass and relative abundance at the community level within the two groups of bivalve species distributed in subtropical or temperate latitudes, and we interpreted the results considering the depth distribution of each species.

Pseudoneilonella pusio is instead more common in the Early–Middle Pleistocene Mediterranean (Dominici and Danise, 2023; La Perna, 2003, 2007), and thus assigned to both subtropical and temperate affinities. *Bathyarca* cf. *philippiana* and *Ennucula* cf. *corbuloides* were assigned the ecological data of *Bathyarca philippiana* and *Ennucula corbuloides*, respectively. The affinities of *Limopsis aurita* were used for *Limopsis* sp. The affinities of *Yoldiella striolata* were used for *Yoldiella* sp. because that was the only species present in the same stratigraphic level. Bivalve specimens identified only to Family level were excluded from this analysis (see supplementary material).

Table 2
Absolute abundances (and relative abundances in brackets) of the identified bivalve taxa in Lardos. Median biomasses (mg) in bold for the most abundant taxa (where they can be calculated).

Taxa	MIS22	MIS21	MIS20	MIS19	MIS18
Acar clathrata			1(0.06)		
Anomiidae indet.				2(0.43)	
Asperarca nodulosa	1(0.51)		1(0.06)		1(0.52)
Bathyarca cf. *philippiana*	4(2.05)	19(1.02)	54(3.06)	23(4.91)	36
	0.0032	**0.0129**	**0.1290**	**0.0034**	(18.85)
					0.0055
Bathyarca pectunculoides	4(2.05)	13(0.70)	85(4.82)	32(6.90)	
		0.0114	**0.0045**	**0.0025**	
Bathyarca philippiana			72(4.08)	4(0.86)	
			0.1290	**0.0034**	
Bathyspinula excisa		4(0.21)	13(0.77)	3(0.65)	
Cyclopecten hoskynsi	1(0.51)		1(0.06)		5(2.62)
Delectopecten vitreus			15(0.89)		4(2.09)
Ennucula cf. *corbuloides*	2(1.03)	3(0.16)	7(0.41)		2(1.05)
Kelliella miliaris	132	821	206	204	76
	(67.69)	(44.09)	(12.17)	(43.97)	(39.79)
	0.0017	**0.0027**	**0.0030**	**0.0027**	**0.0039**
Limatula gwyni	1(0.51)	5(0.27)		5(1.08)	11
					(5.76)
Limatula subauriculata			25(1.48)		
Limea crassa	1(0.51)	6(0.59)	34(1.71)	54(3.88)	12
	0.0257	**0.0178**	**0.0113**	**0.0063**	(13.61)
					0.0069
Limopsis aurita	38	957	684	76	14
	(19.49)	(51.40)	(40.43)	(16.38)	(7.33)
	0.0514	**0.0107**	**0.0064**	**0.0019**	**0.0063**
Limopsis sp.			503		
			(29.73)		
Microgloma sp.				46(9.91)	
				0.0009	
Pseudoneilonella pusio			1(0.06)		
Tellinidae indet.			1(0.06)		
Yoldia minima			6(0.35)		
Yoldiella curta	10(5.13)	11(0.59)	29(1.71)	18(3.88)	26
	0.0045	**0.0051**	**0.0065**	**0.0052**	(13.61)
					0.0066
Yoldiella lucida	1(0.51)	23(1.24)		1(0.22)	
	0.0024	**0.0045**		**0.0589**	
Yoldiella micrometrica			11(0.65)		
Yoldiella philippiana			15(0.89)		
Yoldiella sp.					3(1.57)
Yoldiella striolata					1(0.52)

2.4. Statistical analyses

The relative abundance and size distribution of the bivalves was examined across the studied mean cold and mean warm intervals for the entire assemblage and for the four most abundant species. The Kruskal-Wallis test followed by a pairwise Wilcoxon test with an a posteriori Bonferroni correction (Bonferroni, 1936; Kruskal and Wallis, 1952) was used to compare the mean, the median and the variance in the biomass values and estimate their 95% confidence intervals around this parameter using a bootstrap procedure with 10,000 iterations. All analyses were performed in R (version 4.1.0) (R Core Team, 2019).

3. Results

The bivalve communities in the five MIS intervals include 20 bivalve species: the dominant species are *Limopsis aurita* and *Kelliella miliaris*, while *Limea crassa, Yoldiella curta, Bathyarca pectunculoides* and *Bathyarca philippiana* (incl. *B.* cf. *philippiana*) are very abundant in some levels (Table 2). The shells are small but generally well-preserved. There are no dissolution signs, but marks of drilling predation are occasionally present. Because the shells are quite thin, fragmentation is common. It is possible to measure all three dimensions (*A*, *T* and *D*) in 2547 of the total 4480 specimens collected. The frequency distributions of the shell dimensions are positively skewed with one mode, apart from the level MIS 22 where second modes at larger values are evident (Fig. 4).

Biomass at the community level (Fig. 5) differs significantly between MIS groups ($\chi^2 = 140.7$, df = 4, $p < 2.2e\text{-}16$). The pairwise comparisons shows significant differences specifically between MIS 22 and MIS 21 (biomass median increases from 0.0024 mg to 0.0054 mg), MIS 20 and MIS 19 (decrease from 0.0056 mg to 0.0028 mg), and MIS 19 and MIS 18 (increase from 0.0028 mg to 0.0063 mg). Looking at the dominant species the size-frequency distribution of *Limopsis aurita* shows much greater variance and number of modes than that of *Kelliella miliaris* in all climate cycles, and the median decreases substantially over time until MIS 19 and increases only in MIS 18 (Fig. 5).

The median biomasses of the most abundant species in the assemblages display contrasting patterns across the studied time interval (Fig. 6). The median biomass of *K. miliaris* increases from 0.0017 mg in MIS 22 to 0.0039 mg in MIS 18 ($\chi^2 = 93.614$, df = 4, $p < 2.2e\text{-}16$; significant increases from MIS 22 to MIS 21 and from MIS 19 to MIS 18 based on the pairwise comparison). The median biomass of *Limopsis aurita* decreases significantly from 0.0514 mg in MIS 22 to 0.0063 in MIS 18 ($\chi^2 = 83.346$, df = 4, $p < 2.2e\text{-}16$; significant change from MIS 22 to MIS 21 and from MIS 20 to MIS 19), but the observed increase in MIS 18 (Fig. 6) is not significant ($p = 0.22176$). *Limea crassa* has a median biomass of 0.0257 mg in MIS 22 that decreases to 0.0063 mg in MIS 19, but this difference is not very significant ($\chi^2 = 16.82$, df = 4, $p = 0.002$). The median biomass of *Bathyarca philippiana* decreases from 0.0129 in MIS 20 to 0.0034 in MIS 19 ($\chi^2 = 23.321$, df = 4, $p = 0.0001$; the increase in MIS 18 is not significant). The changes observed for *Yoldiella curta, Bathyarca penctuculoides, Yoldiella lucida* and *Microgloma* sp. are not significant because of the low number of specimens in most climate cycles (their median biomasses, where calculated, are shown in Table 2).

The most abundant families within the whole assemblage are Limopsidae, Kelliellidae (represented only by *K. miliaris*), Arcidae and Yoldiidae (Fig. 7). Limopsidae, which include here the specimens identified as *Limopsis aurita* and those assigned to *Limopsis* sp., confirm the biomass decreasing pattern observed for *L. aurita*. Arcidae are represented by *Acar clathrata, Asperarca nodulosa, Bathyarca pectunculoides* and *Bathyarca philippiana*. The median biomass of this family decreases from MIS 20 to MIS 19 ($\chi^2 = 41.955$, df = 4, $p = 2.8e\text{-}07$) and then increases in MIS 18 ($p = 0.0005$). Yoldiidae are represented by *Yoldia minima, Yoldiella curta, Yoldiella lucida, Yoldiella micrometrica, Yoldiella philippiana* and *Yoldiella striolata*. The median biomass of this family does not show significant variation in MIS 22–18 ($\chi^2 = 14.755$, df = 4, $p = 0.005$).

The bivalve assemblages are dominated by temperate taxa (Fig. 8). The median biomass of the temperate group increases from MIS 22 to MIS 21 ($\chi^2 = 102.86$, df = 4, $p = 9.3e\text{-}06$), then decreases from MIS 20 to MIS 19 ($p = 2.8e\text{-}15$), and then increases again from MIS 19 to MIS 18 ($p = 3.7e\text{-}16$). The median biomass of the subtropical group shows similar changes, but they are smaller in amplitude and only the shifts from MIS 20 to MIS 19 ($\chi^2 = 54.349$, df = 4, $p = 3.5e\text{-}11$) and from MIS 19 to MIS 18 ($p = 2.6e\text{-}05$) are significant. The lack of significant results for the subtropical group for the MIS 22–21 comparison may result from the low abundance of this group in MIS 21 (Fig. 8).

The median biomass of the epifaunal group changes significantly throughout the studied interval (Fig. 9; $\chi^2 = 85.565$, df = 4, $p < 2.2e\text{-}16$). It decreases from MIS 22 to MIS 21 ($p = 6.8e\text{-}0.7$), while their relative abundance increases. From MIS 20 to MIS 19, both their median biomass ($p = 8.1e\text{-}06$) and abundance decrease. The median biomass of the epifaunal group increases again in MIS 18 ($p = 7.7e\text{-}05$), but the relative abundance remains unchanged. Although the observed changes in median biomass for the infaunal group are milder, they are significant ($\chi^2 = 186.52$, df = 4, $p < 2.2e\text{-}16$). Indeed, there is an increase in median biomass from MIS 22 to MIS 21 ($p < 2e\text{-}16$), a decrease from MIS 20 to MIS 19 ($p = 4e\text{-}13$), and again an increase to MIS 18 ($p < 2e\text{-}16$).

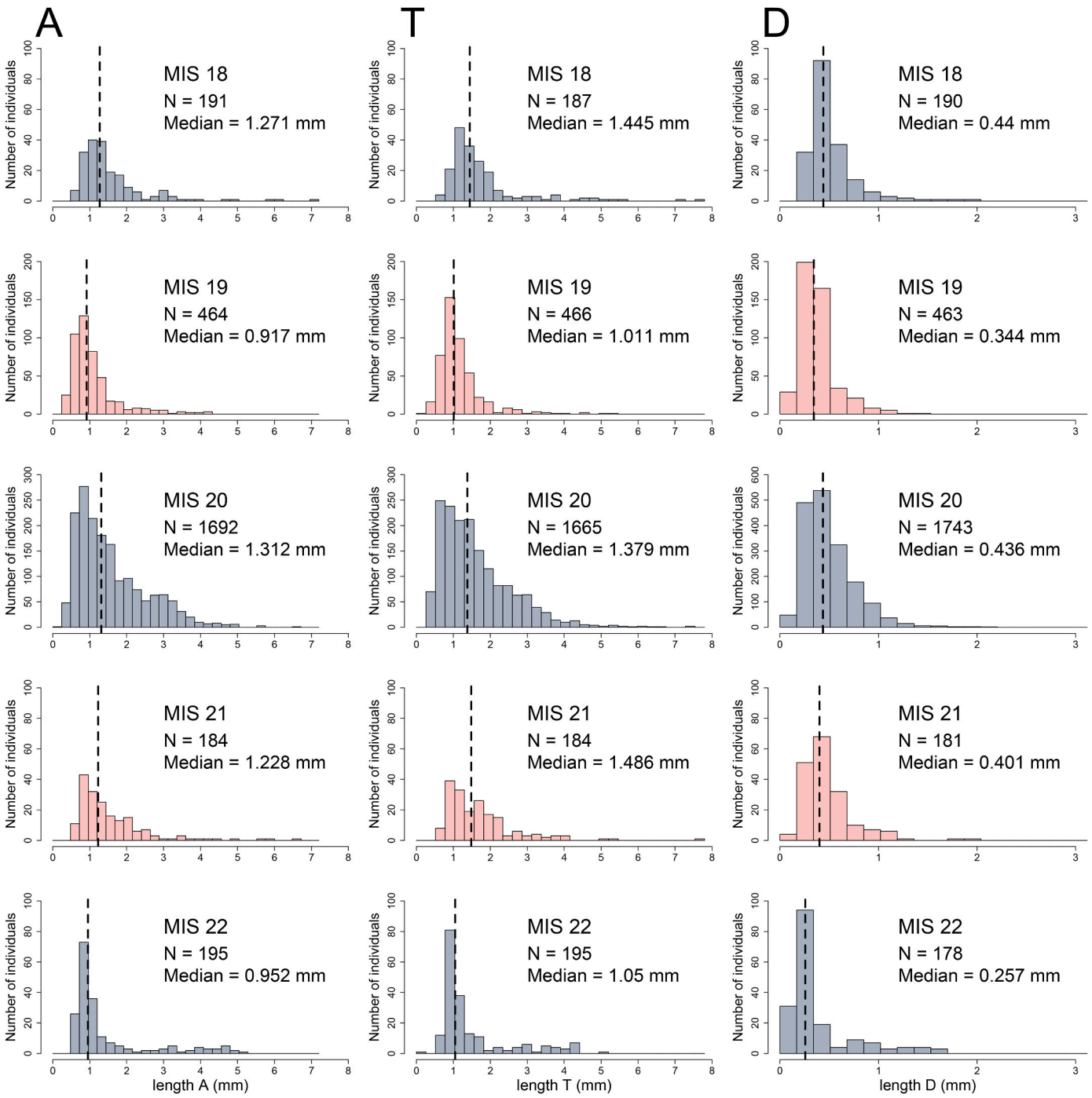

Fig. 4. Frequency distributions of the bivalves antero-posterior length (A), transversal length (T), and depth (D) in MIS 22, 20 and 18 (colder) and MIS 21 and 19 (warmer intervals).

4. Discussion

4.1. Shell preservation

Size-frequency distributions from fossil shells can be influenced by differences in host sediment lithology, changes in sedimentation rate and seawater chemistry, all affecting the state of preservation of the shells, potentially favoring larger individuals through the dissolution of small shells (Behrensmeyer et al., 2000; Huang et al., 2023; Mukhopadhyay et al., 2023). Shells of *Kelliella miliaris* are characteristically thin and therefore more prone to fragmentation and complete dissolution (Sorensen, 1984). The absence of dissolution marks and the high abundance of well-preserved small shells of *Kelliella miliaris* in all stratigraphic levels (Fig. 6) indicates that preferential dissolution and fragmentation was not an issue in the case of the bivalve fossil assemblages from Lardos.

4.2. Age model and study limitations

Evaluating a potential relationship between seawater temperature and body size in a paleoceanographic setting depends on the quality of the chronostratigraphic framework and the sampling resolution. In the present study, because our goal was to examine individual biomass changes at species-as well as community-level, large volumes of

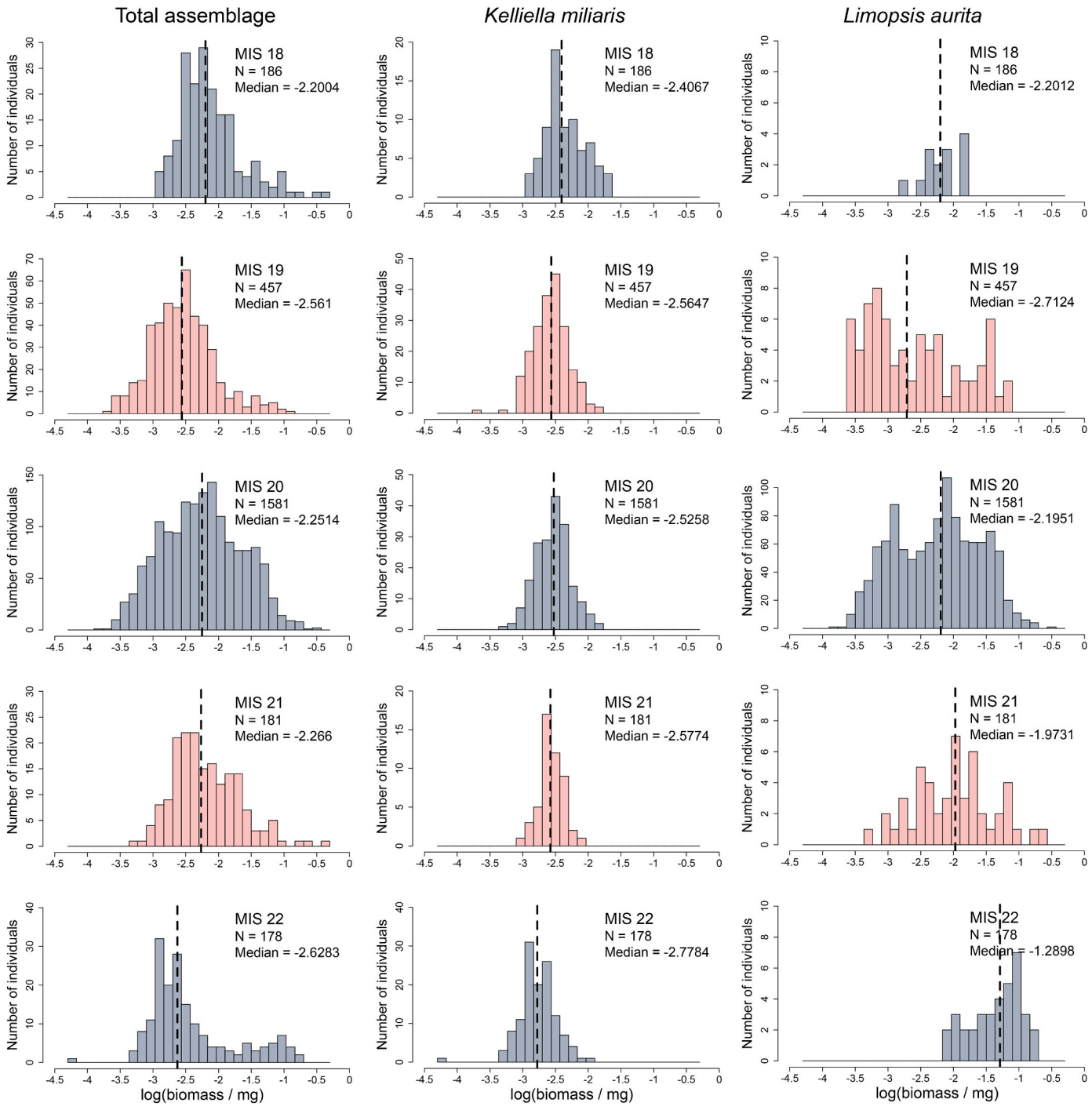

Fig. 5. Bivalve frequency distribution of individual biomass (log-transformed) in MIS 22, 20 and 18 (colder) and MIS 21 and 19 (warmer) intervals for the total assemblage (left column) and the two most abundant species *Kelliella miliaris* (middle column) and *Limopsis aurita* (right column).

sediment were required and collected within thin stratigraphic intervals (Fig. 2). Consequently, it was not possible to obtain a finer stratigraphic resolution than at the level of entire MIS, and we could not distinguish between stadials and interstadials within MIS. Furthermore, the available age model by Titschack et al. (2013) does not allow distinguishing between stadials and interstadials within the sampled marine isotope stages. This is the main limitation of our results, which ultimately gives an overall picture of mean cold versus mean warm conditions. For example, in MIS 18, it is very likely that our sample, which was centered in the MIS interval, mainly captured MIS 18b–d, which was a warmer interstadial phase (Konijnendijk et al., 2015; Martin-Garcia et al., 2015; Quillévéré et al., 2019; Rodrigues et al., 2017). This may explain why high relative abundance of subtropical bivalves (this work) and fish (Agiadi et al., 2023) were found in the MIS 18 sample.

4.3. *Species size-frequency distributions as indicators of population structure*

Fossil-based size-frequency distributions can inform about changes in growth and mortality rates of a species throughout the sampled time-interval, although absolute estimates of these rates cannot be established without prior knowledge of either growth or mortality. The

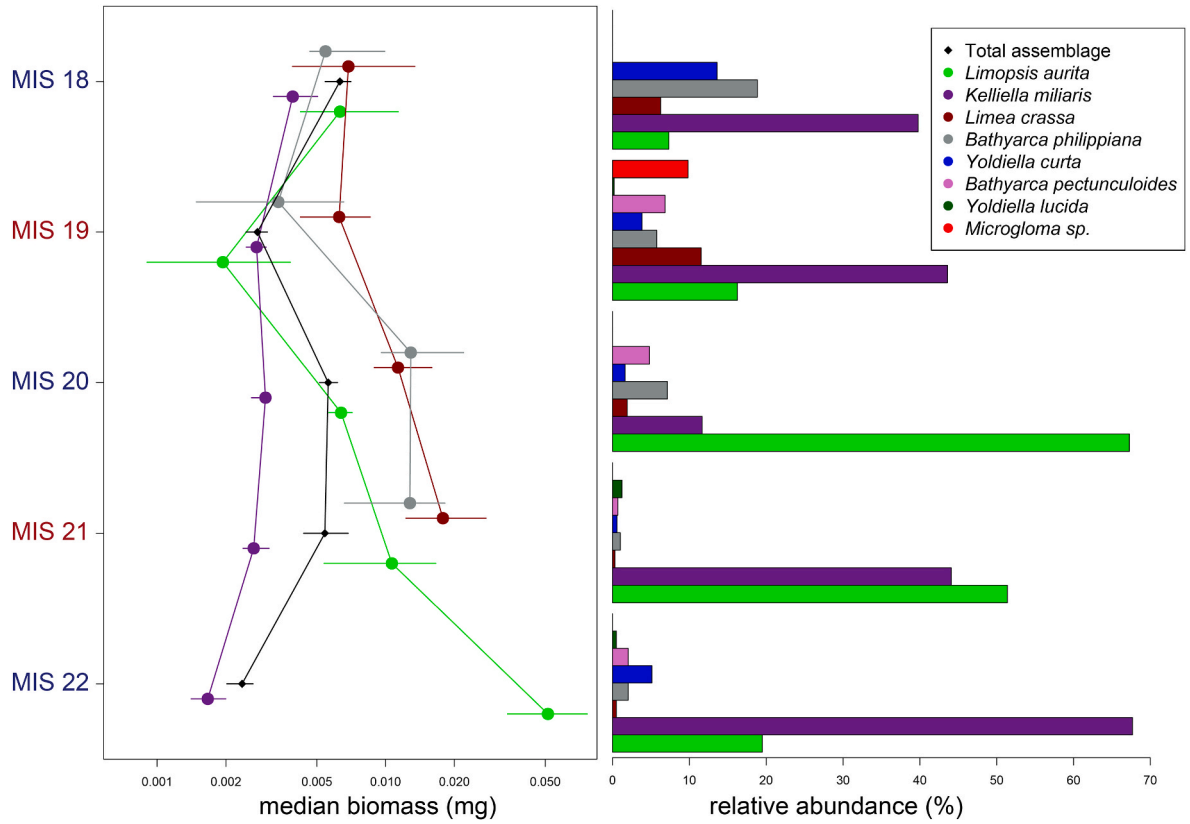

Fig. 6. Median biomass (mg) with 95% confidence interval and relative abundance (%) of the most abundant species and of the total assemblage over the five studied climate cycles. Only significant biomass patterns are shown.

logarithmic shape of the size-frequency curve for *K. miliaris* is consistent with that previously observed by Sorensen (1984), which therefore indicates a stable population structure within each of the investigated climate cycles. In contrast, the size-frequency curves for *L. aurita* do not show any consistency, neither in range nor in shape or number of peaks, suggesting that the population structure has strongly fluctuated in the studied interval. Both species are distributed from the euphotic zone down to depths >1000 m, but *K. miliaris* is an infaunal species, whereas *L. aurita* is epifaunal and therefore more susceptible to warming and deoxygenation (Kruft Welton et al., 2023). In this case, however, the water column was oxygenated during both MIS 21 and MIS 19 (Emeis et al., 2000; Grant et al., 2022), and the paleodepth (maximum at 250 m; Agiadi et al., 2018) was too shallow, implying mixing. Therefore, we can only consider a possible effect of warming in destabilizing the *L. aurita* population structure.

4.4. Examining the validity of the temperature–size rule

In the eastern Mediterranean, the trajectories for biomass expected based on the temperature–size rule are not observed in MIS 22–18 neither at species nor at family level (Figs. 6 and 7). Along with changes in phenology (Durant et al., 2007; Walther et al., 2002) and distribution range shifts (Crippa et al., 2016; Meadows et al., 2019; Parmesan and Yohe, 2003), reduced biomass is proposed to be a universal reaction to climate warming in aquatic systems (Daufresne et al., 2009; Ohlberger, 2013). Smaller biomass during warmer intervals would be explained by the temperature–size rule, which states that an increase in temperature should result in a decrease in individual biomass for ectotherms: the size decrease manifests as a shift in size-at-age within a community, due to differences in the thermal sensitivity of both developmental and growth rates within an organism (Atkinson, 1994). Notably, the generality of the temperature–size rule across the Cenozoic has been challenged, at least for bivalves of the continental shelf (Chattopadhyay and Chattopadhyay, 2020). Our results show that in the eastern Mediterranean, bathyal bivalves did not respond uniformly to the temperature increases that should have occurred from colder to warmer intervals of the Early–Middle Pleistocene Transition.

4.5. Biodiversity impact on community-level biomass

The median biomass of bivalves in the assemblages is driven by the relative abundances of the species (Figs. 5 and 7). The bivalve shells in the Lardos assemblages are overall relatively small, with A_{min} = 0.02 mm and A_{max} = 7.75 mm) (Fig. 4), whereas in modern environments, *L. aurita* reaches an A_{max} of 15 mm (Rosenberg, 2009) and *K. miliaris* of 3 mm (Passos et al., 2019), but *L. crassa* A_{max} can be as large as 55 mm (Allen, 2004). *Kelliella miliaris* (the smallest of the most abundant species in our assemblages) often drives the median shell biomass at the community level to smaller values. However, the gradually increasing trend in the biomass of *K. miliaris* is counteracted in MIS 21 and MIS 20 by the large biomass values of *L. aurita* that shows high relative abundances in those intervals, since *L. aurita* shells are comparatively much larger (Fig. 6). Indeed, the shell biomass of *K. miliaris* increases significantly during the MIS 22–21 climate transition, whereas it remains the same during the MIS 20–19 transition, probably counteracting the effects of strong climatic variability that are affecting the other bivalve species (see discussion below) and other marine organisms (Agiadi et al., 2018, 2023; Marino et al., 2020b; Quillévéré et al., 2019; Quivelli et al., 2020). Additionally, based on the records from the western Iberian margin, the MIS 22–21 climate transition lasted longer than that of MIS20–19 (Bajo et al., 2020; Martin-Garcia et al., 2015; Rodrigues et al., 2017), implying greater resilience of *K. miliaris* to climatic variability. In contrast, the shell biomass of the larger species *L. aurita* decreases during the MIS 22–21 and MIS 20–19 transitions along with its abundance.

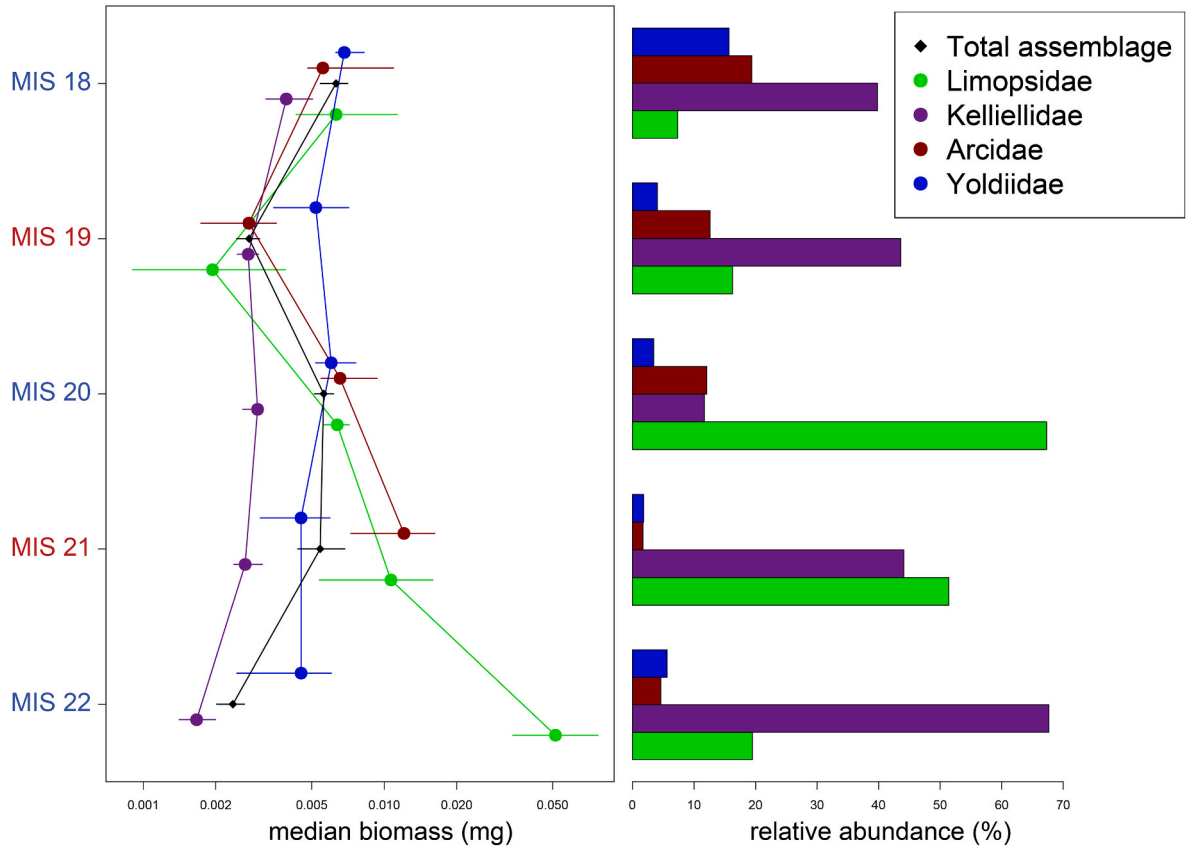

Fig. 7. Median biomass (mg) with 95% confidence interval and relative abundance (%) of the most dominant families over the five studied climate cycles. Only significant biomass patterns are shown.

4.6. Bivalve biomass distribution: biotic factors

For suspension-feeding bivalves, food supply and hence primary productivity play an important role on their growth (Bonsdorff and Blomqvist, 1993; Gili and Coma, 1998). High nutrient supply and primary productivity has been evidenced for the central and western Mediterranean in interglacial MIS 19 (at least its early part, MIS 19c) compared to glacial MIS 20 (Maiorano et al., 2021; Marino et al., 2022; Nomade et al., 2019; Quivelli et al., 2020). Potentially, increased recruitment across the species in the community may explain the smallest median biomass overall (Fig. 6), and it is supported by the more even community and the great variance of biomass of *Limopsis aurita* in that interval (Fig. 5).

Larger bivalve species shifted their geographical range more often and by a greater amount than smaller species in response to climate cycles (Roy et al., 2001). Consequently, changes in temperature led to shifts in community composition: as larger species migrated to new habitats, the relative abundance of smaller taxa in the community increased. The resulting community therefore exhibits a smaller median biomass. This explains the more dynamic pattern in the relative abundance and median biomass of the larger species *Limopsis aurita* compared to the smaller *Kelliella miliaris* (Fig. 6).

4.7. Bivalve biomass distribution: abiotic factors

Although the median biomass of the bivalve assemblage and taxa does not decrease consistently from colder to warmer intervals, a decrease in median biomass is observed for all species between MIS 20 and MIS 19 (Fig. 6). The studied interval captures the end of the EMPT, which was characterized by large glacial ice-sheets, warm North Atlantic sea surface temperatures, and increased moisture input to the Mediterranean region from both the Atlantic and the South East Asian Monsoon system (Berends et al., 2021; Elderfield et al., 2012; Head, 2021; Head and Gibbard, 2015; Pena and Goldstein, 2014; Rohling et al., 2014; Sánchez Goñi et al., 2023). The MIS 20–19 transition was not very strong, and the whole interval was characterized by millennial-scale variability that has been associated with disruptions to the Atlantic Meridional Oceanic Circulation (AMOC) (Hodell et al., 2023; Hodell and Channell, 2016) and has been particularly well-recorded in the Mediterranean (Haneda et al., 2020; Maiorano et al., 2016; Martin-Garcia et al., 2018; Nomade et al., 2019). Across the Mediterranean, high-amplitude millennial-scale variability in seawater temperatures, salinities and circulation have been evidenced (Konijnendijk et al., 2015; Quivelli et al., 2021) with impacts on marine plankton (Marino et al., 2020a; Quillévéré et al., 2019), but also on deep-water organisms such as mesopelagic fishes (Agiadi et al., 2018, 2023). Because sea bottom temperatures remained stable between glacials of the EMPT in the Mediterranean (Peral et al., 2020), absolute seawater temperature values during MIS 20 cannot account for the observed changes neither in the bivalve assemblage compositions nor on the bivalve biomasses (Fig. 6). The increase in the relative abundance of subtropical taxa and the stronger decrease in the median biomass in MIS 19 (Fig. 8) may instead be explained by the recurring millennial-scale variability that occurred during MIS 20–19 (Bajo et al., 2020; Naafs et al., 2011; Quillévéré et al., 2019; Quivelli et al., 2021; Rodrigues et al., 2017), which is beyond the resolution of this study.

In addition to temperature, the carbon and oxygen supplies can also play a significant role as first-order drivers of biomass (Bryant and McClain, 2022). Since a positive correlation between dissolved oxygen concentration and maximum size in marine molluscs has been evidenced elsewhere (McClain and Rex, 2001), locally low-oxygen concentrations, even at shallow water depths (40–140 m) (Rossi et al., 2018), may have

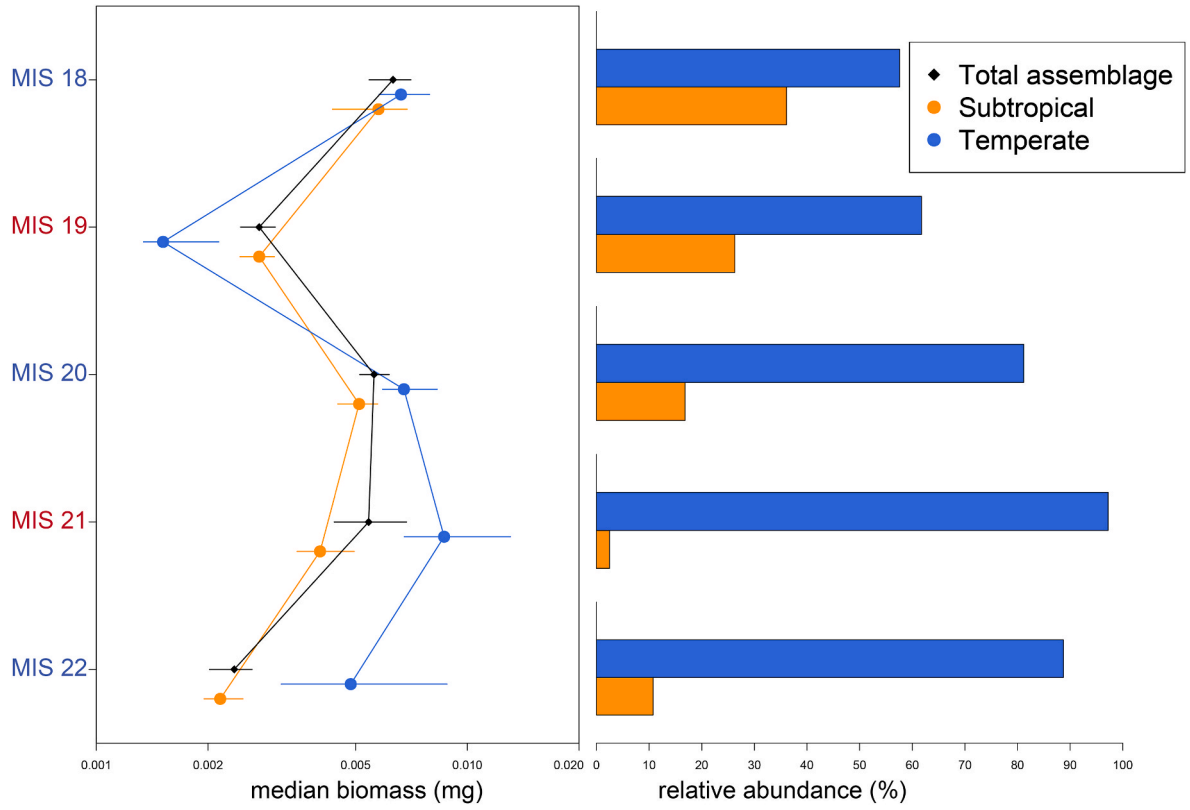

Fig. 8. Median biomass (mg) with 95% confidence interval and relative abundance (%) of the bivalve species grouped based on their climatic distributions in the five studied climate cycles.

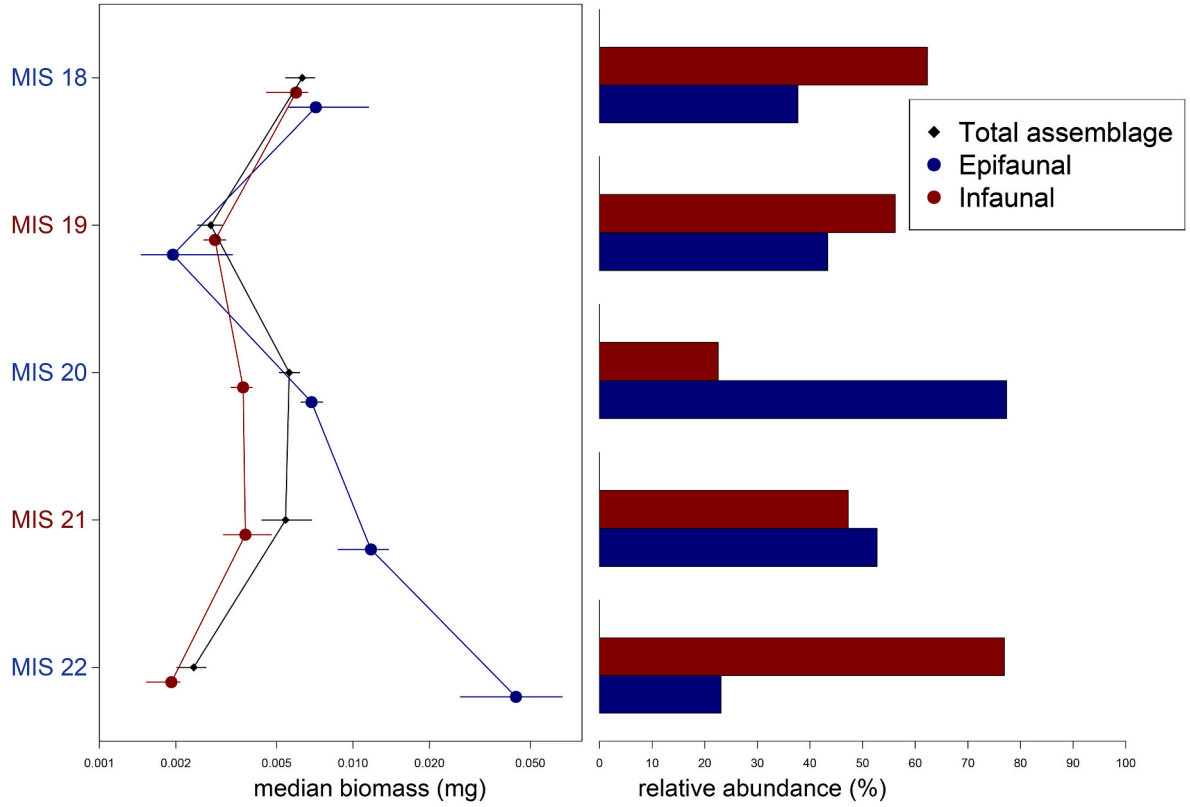

Fig. 9. Median biomass (mg) with 95% confidence interval and relative abundance (%) of the epifaunal and infaunal taxa in the five studied climate cycles.

reinforced the median biomass reduction that has occurred during MIS 19 (Bryant and McClain, 2022; Payne et al., 2011). Larger species, here *Limopsis aurita*, are more affected by oxygen and resource restrictions because of their metabolic demands (Verberk et al., 2021), while the higher temperatures during the interglacials further increases their oxygen demand. Furthermore, dysoxic conditions in the water column decrease the abundance of primary producers, and thereby food availability for bivalves through bottom-up control (Seitz and Lipcius, 2001), which in turn could restrict growth and lead to a smaller biomass at age. Consequently, oxygen supply may have played an important role in the observed biomass trends during the warmer MIS 19. However, as discussed in 4.6, the increased recruitment of bivalves in MIS 19, which also explains the smallest median biomass (Fig. 6), is better supported here.

Changes in oceanic circulation and sea bottom ventilation have a stronger impact on epifaunal and shallow infaunal, rather than deeper infaunal organisms that are less susceptible to the conditions on the sea floor. The observed changes in median shell biomass of the epifaunal group are much stronger throughout the studied interval, although the milder changes observed in the infaunal group are statistically significant (Fig. 9). In the central Mediterranean, interglacials MIS 21 and MIS 19 have been associated with decreased ventilation of the sea floor (Rossi et al., 2018). On the other hand, thermohaline circulation was probably well-active at that time, resulting in enhanced Mediterranean outflow water to the Atlantic (Guo et al., 2020). The decreased shell biomasses for both epifauna and infauna in MIS 19 (Fig. 9) suggest that the bottom-water environment in the eastern Mediterranean was more unstable in MIS 19 than in MIS 21, when only epifaunal taxa were affected.

5. Conclusions

Over the MIS 22–18 targeted time interval of the EMPT, no consistency in the trajectories of biomass changes could be found for all taxa and climatic-affinity groups that could be solely attributed to the influence of ambient water temperature. Various biotic and abiotic factors ultimately affect shell biomass across important Earth System transitions, such as variations in productivity and oxygen variability, whose contributions should be examined using independent proxies. The results of this study highlight the complexity of morphological changes in marine mollusc communities, particularly those triggered or induced by climatic alterations. The shell biomass of larger species appears more susceptible to climate change. The interplay between relative abundance and shell biomass-frequency distribution determine bivalve biomass at the community level: smaller species are not necessarily favored, but larger species seem to be most affected by climate warming.

CRediT authorship contribution statement

Antonia Porz: Formal analysis, Funding acquisition, Writing – original draft. **Martin Zuschin:** Funding acquisition, Investigation, Writing – review & editing. **Luke Strotz:** Formal analysis, Writing – original draft. **Efterpi Koskeridou:** Investigation, Writing – review & editing. **Kobe Simoens:** Formal analysis, Writing – review & editing. **Renata Lukić:** Formal analysis, Writing – review & editing. **Danae Thivaiou:** Investigation, Writing – review & editing. **Frédéric Quillévéré:** Funding acquisition, Investigation, Writing – review & editing. **Konstantina Agiadi:** Conceptualization, Formal analysis, Funding acquisition, Investigation, Methodology, Project administration, Supervision, Writing – original draft.

Declaration of competing interest

The authors declare that they have no known competing financial interests or personal relationships that could have appeared to influence the work reported in this paper.

Data availability

All data produced in this study are made available in the supplementary material.

Acknowledgements

The authors would like to thank the two anonymous reviewers for their very constructive and helpful comments. This work was funded by the Austrian Science Fund (FWF) project M2894-N “Deep-time climate change impact on marine food webs” (P.I.: KA). AP was supported by the “Haus des Meeres” through the “Rupert-Riedl-Stipendium”. FQ was supported by the National programs Tellus-INTERRVIE and Tellus-SYSTER of CNRS-INSU. The authors would like to acknowledge Jean-Jacques Cornée and Pierre Moissette for showing us the Lardos section and for the insightful discussions on the geology of Rhodes. We would like to thank George Kontakiotis and Vasiliki Lianou for their help during fieldwork. This research contributes to the objectives of Q-MARE (a PAGES working group).

Appendix A. Supplementary data

Supplementary data to this article can be found online at https://doi.org/10.1016/j.dsr.2023.104224.

References

Agiadi, K., Girone, A., Koskeridou, E., Moissette, P., Cornée, J.-J., Quillévéré, F., 2018. Pleistocene marine fish invasions and paleoenvironmental reconstructions in the eastern Mediterranean. Quat. Sci. Rev. 196, 80–99. https://doi.org/10.1016/j.quascirev.2018.07.037.

Agiadi, K., Quillevere, F., Nawrot, R., Sommeville, T., Coll, M., Koskeridou, E., Fietzke, J., Zuschin, M., 2023. Palaeontological evidence for community-level decrease in mesopelagic fish size during Pleistocene climate warming in the eastern Mediterranean. Proc. R. Soc. B-Biol. Sci. 290 https://doi.org/10.1098/rspb.2022.1994.

Agiadi, K., Triantaphyllou, M., Girone, A., Karakitsios, V., 2011. The early Quaternary palaeobiogeography of the eastern Ionian deep-sea Teleost fauna: a novel palaeocirculation approach. Palaeogeogr. Palaeoclimatol. Palaeoecol. 306, 228–242. https://doi.org/10.1016/j.palaeo.2011.04.029.

Allen, J.A., 2004. The Recent species of the genera Limatula and Limea (Bivalvia, Limacea) present in the Atlantic, with particular reference to those in deep water. J. Nat. Hist. 38, 2591–2653. https://doi.org/10.1080/00222930310001647442.

Atkinson, D., 1995. Effects of temperature on the size of aquatic ectotherms: Exceptions to the general rule. J. Therm. Biol., Effects of Rising Temperature on the Ecology and Physiology of Aquatic Organisms 20, 61–74. https://doi.org/10.1016/0306-4565(94)00028-H.

Atkinson, D., 1994. Temperature and organism size—a Biological Law for ectotherms? In: Begon, M., Fitter, A.H. (Eds.), Advances in Ecological Research. Academic Press, pp. 1–58. https://doi.org/10.1016/S0065-2504(08)60212-3.

Audzijonyte, A., Richards, S.A., Stuart-Smith, R.D., Pecl, G., Edgar, G.J., Barrett, N.S., Payne, N., Blanchard, J.L., 2020. Fish body sizes change with temperature but not all species shrink with warming. Nat. Ecol. Evol. 4, 809–814. https://doi.org/10.1038/s41559-020-1171-0.

Bajo, P., Drysdale, R.N., Woodhead, J.D., Hellstrom, J.C., Hodell, D., Ferretti, P., Voelker, A.H.L., Zanchetta, G., Rodrigues, T., Wolff, E., Tyler, J., Frisia, S., Spötl, C., Fallick, A.E., 2020. Persistent influence of obliquity on ice age terminations since the Middle Pleistocene transition. Science 367, 1235–1239. https://doi.org/10.1126/science.aaw1114.

Behrensmeyer, A.K., Kidwell, S.M., Gastaldo, R.A., 2000. Taphonomy and paleobiology. Paleobiology 26, 103–147. https://doi.org/10.1017/S0094837300026907.

Berends, C.J., Köhler, P., Lourens, L.J., van de Wal, R.S.W., 2021. On the Cause of the mid-Pleistocene transition. Rev. Geophys. 59, e2020RG000727 https://doi.org/10.1029/2020RG000727.

Bonferroni, C., 1936. Teoria statistica delle classi e calcolo delle probabilita. Pubblicazioni R Ist. Super. Sci. Econ. E Commericiali Firenze 8, 3–62.

Bonsdorff, E., Blomqvist, E., 1993. Biotic coupling on shallow water soft bottoms – examples from the Northern Baltic Sea. Oceanogr. Mar. Biol. Annu. Rev. 31, 31.

Bryant, S.R.D., McClain, C.R., 2022. Energetic constraints on body-size niches in a resource-limited marine environment. Biol. Lett. 18, 20220112 https://doi.org/10.1098/rsbl.2022.0112.

Caswell, B.A., Coe, A.L., 2013. Primary productivity controls on opportunistic bivalves during Early Jurassic oceanic deoxygenation. Geology 41, 1163–1166. https://doi.org/10.1130/G34819.1.

Ceregato, A., Raffi, S., Scarponi, D., 2007. The circalittoral/bathyal paleocommunities in the Middle Pliocene of Northern Italy: the case of the Korobkovia oblonga–Jupiteria concava paleocommunity type. Geobios 40, 555–572. https://doi.org/10.1016/j.geobios.2006.08.004.

Chattopadhyay, Debarati, Chattopadhyay, Devapriya, 2020. Absence of general rules governing molluscan body-size response to climatic fluctuation during the Cenozoic. Hist. Biol. 32, 1071–1080. https://doi.org/10.1080/08912963.2018.1563894.

Cornée, J.-J., Moissette, P., Joannin, S., Suc, J.-P., Quillévéré, F., Krijgsman, W., Hilgen, F., Koskeridou, E., Münch, P., Lécuyer, C., Desvignes, P., 2006. Tectonic and climatic controls on coastal sedimentation: the late Pliocene–middle Pleistocene of northeastern Rhodes, Greece. Sediment. Geol. 187, 159–181. https://doi.org/10.1016/j.sedgeo.2005.12.026.

Cornée, J.-J., Quillévéré, F., Moissette, P., Fietzke, J., López-Otálvaro, G.E., Melinte-Dobrinescu, M., Philippon, M., Hinsbergen, D.J.J. van, Agiadi, K., Koskeridou, E., Münch, P., 2019. Tectonic motion in oblique subduction forearcs: insights from the revisited Middle and Upper Pleistocene deposits of Rhodes, Greece. J. Geol. Soc. 176, 78–96. https://doi.org/10.1144/jgs2018-090.

Crippa, G., Angiolini, L., Bottini, C., Erba, E., Felletti, F., Frigerio, C., Hennissen, J.A.I., Leng, M.J., Petrizzo, M.R., Raffi, I., Raineri, G., Stephenson, M.H., 2016. Seasonality fluctuations recorded in fossil bivalves during the early Pleistocene: implications for climate change. Palaeogeogr. Palaeoclimatol. Palaeoecol. 446, 234–251. https://doi.org/10.1016/j.palaeo.2016.01.029.

Danise, S., Dominici, S., 2023. Biodiversity change and extinction risk in plio-Pleistocene Mediterranean bivalves: the families Veneridae, Pectinidae and Lucinidae. Geol. Soc. Lond. Spec. Publ. 529 https://doi.org/10.1144/SP529-2022-44. SP529-2022–44.

Daufresne, M., Lengfellner, K., Sommer, U., 2009. Global warming benefits the small in aquatic ecosystems. Proc. Natl. Acad. Sci. 106, 12788–12793. https://doi.org/10.1073/pnas.0902080106.

Delongueville, C., Scaillet, R., Swinnen, F., 2019. New records of marine littoral Gastropoda and Bivalvia in the Azores archipelago (Northeast Atlantic Ocean). NOVAPEX 20, 35–43.

Dietl, G.P., Kidwell, S.M., Brenner, M., Burney, D.A., Flessa, K.W., Jackson, S.T., Koch, P. L., 2015. Conservation paleobiology: Leveraging knowledge of the past to inform Conservation and Restoration. Annu. Rev. Earth Planet Sci. 43, 79–103. https://doi.org/10.1146/annurev-earth-040610-133349.

Dobzhansky, T., 1950. Evolution in the Tropics.

Dominici, S., Danise, S., 2023. Mediterranean onshore–offshore gradient in the composition and temporal turnover of benthic molluscs across the middle Piacenzian Warm Period. Geol. Soc. Lond. Spec. Publ. 529, 365–394. https://doi.org/10.1144/SP529-2022-35.

Durant, J., Ottersen, G., Stenseth, N.C., 2007. Climate and the match or mismatch between predator requirements and resource availability. Clim. Res. 33, 271–283. https://doi.org/10.3354/cr033271.

Elderfield, H., Ferretti, P., Greaves, M., Crowhurst, S., McCave, I.N., Hodell, D., Piotrowski, A.M., 2012. Evolution of ocean temperature and ice volume through the mid-Pleistocene climate transition. Science 337, 704–709. https://doi.org/10.1126/science.1221294.

Emeis, K.-C., Sakamoto, T., Wehausen, R., Brumsack, H.-J., 2000. The sapropel record of the eastern Mediterranean Sea — results of ocean drilling program Leg 160. Palaeogeogr. Palaeoclimatol. Palaeoecol. 158, 371–395. https://doi.org/10.1016/S0031-0182(00)00059-6.

Estes, J.A., Terborgh, J., Brashares, J.S., Power, M.E., Berger, J., Bond, W.J., Carpenter, S.R., Essington, T.E., Holt, R.D., Jackson, J.B.C., Marquis, R.J., Oksanen, L., Oksanen, T., Paine, R.T., Pikitch, E.K., Ripple, W.J., Sandin, S.A., Scheffer, M., Schoener, T.W., Shurin, J.B., Sinclair, A.R.E., Soulé, M.E., Virtanen, R., Wardle, D.A., 2011. Trophic Downgrading of Planet Earth. Science 333, 301–306. https://doi.org/10.1126/science.1205106.

Foster, W.J., Gliwa, J., Lembke, C., Pugh, A.C., Hofmann, R., Tietje, M., Varela, S., Foster, L.C., Korn, D., Aberhan, M., 2020. Evolutionary and ecophenotypic controls on bivalve body size distributions following the end-Permian mass extinction. Glob. Planet. Change 185, 103088. https://doi.org/10.1016/j.gloplacha.2019.103088.

Gili, J.-M., Coma, R., 1998. Benthic suspension feeders: their paramount role in littoral marine food webs. Trends Ecol. Evol. 13, 316–321. https://doi.org/10.1016/S0169-5347(98)01365-2.

Girone, A., De Astis, A., Sierro, F.J., Hernández-Almeida, I., Garcia, M.A., Sánchez Goñi, M.F., Maiorano, P., Marino, M., Trotta, S., Hodell, D., 2023. Planktonic foraminifera response to orbital and millennial-scale climate variability at the southern Iberian Margin (IODP Site U1385) during Marine Isotope Stages 20 and 19. Palaeogeogr. Palaeoclimatol. Palaeoecol. 615, 111450 https://doi.org/10.1016/j.palaeo.2023.111450.

Gobler, C.J., DePasquale, E.L., Griffith, A.W., Baumann, H., 2014. Hypoxia and acidification have additive and Synergistic negative effects on the growth, Survival, and Metamorphosis of early life stage bivalves. PLoS One 9, e83648. https://doi.org/10.1371/journal.pone.0083648.

Grant, K.M., Amarathunga, U., Amies, J.D., Hu, P., Qian, Y., Penny, T., Rodriguez-Sanz, L., Zhao, X., Heslop, D., Liebrand, D., Hennekam, R., Westerhold, T., Gilmore, S., Lourens, L.J., Roberts, A.P., Rohling, E.J., 2022. Organic carbon burial in Mediterranean sapropels intensified during Green Sahara Periods since 3.2 Myr ago. Commun. Earth Environ 3, 1–9. https://doi.org/10.1038/s43247-021-00339-9.

Guo, Q., Li, B., Voelker, A.H.L., Kim, J.-K., 2020. Mediterranean Outflow Water dynamics across the middle Pleistocene transition based on a 1.3 million-year benthic foraminiferal record off the Portuguese margin. Quat. Sci. Rev. 247, 106567 https://doi.org/10.1016/j.quascirev.2020.106567.

Haneda, Y., Okada, M., Kubota, Y., Suganuma, Y., 2020. Millennial-scale hydrographic changes in the northwestern Pacific during marine isotope stage 19: Teleconnections with ice melt in the North Atlantic. Earth Planet Sci. Lett. 531, 115936 https://doi.org/10.1016/j.epsl.2019.115936.

Head, M.J., 2021. Review of the early–middle Pleistocene boundary and marine isotope stage 19. Prog. Earth Planet. Sci. 8, 50. https://doi.org/10.1186/s40645-021-00439-2.

Head, M.J., Gibbard, P.L., 2015. Early–Middle Pleistocene transitions: linking terrestrial and marine realms. Quat. Int., The Jaramillo Subchron and the Early-Middle Pleistocene transition in continental records from a multidisciplinary perspective 389, 7–46. https://doi.org/10.1016/j.quaint.2015.09.042.

Hildrew, A.G., Raffaelli, D.G., Edmonds-Brown, R. (Eds.), 2007. Body Size: the Structure and Function of Aquatic Ecosystems. Ecological Reviews. Cambridge University Press, Cambridge. https://doi.org/10.1017/CBO9780511611223.

Hodell, D.A., Channell, J.E.T., 2016. Mode transitions in Northern Hemisphere glaciation: co-evolution of millennial and orbital variability in Quaternary climate. Clim. Past 12, 1805–1828. https://doi.org/10.5194/cp-12-1805-2016.

Hodell, D.A., Crowhurst, S.J., Lourens, L., Margari, V., Nicolson, J., Rolfe, J.E., Skinner, L.C., Thomas, N.C., Tzedakis, P.C., Mleneck-Vautravers, M.J., Wolff, E.W., 2023. A 1.5-million-year record of orbital and millennial climate variability in the North Atlantic. Clim. Past 19, 607–636. https://doi.org/10.5194/cp-19-607-2023.

Houpert, L., Testor, P., Durrieu de Madron, X., Somot, S., D'Ortenzio, F., Estournel, C., Lavigne, H., 2015. Seasonal cycle of the mixed layer, the seasonal thermocline and the upper-ocean heat storage rate in the Mediterranean Sea derived from observations. Prog. Oceanogr., Oceanography of the Arctic and North Atlantic Basins 132, 333–352. https://doi.org/10.1016/j.pocean.2014.11.004.

Huang, H.-H.M., Yasuhara, M., Iwatani, H., Yamaguchi, T., Yamada, K., Mamo, B., 2019. Deep-sea ostracod faunal dynamics in a marginal sea: biotic response to oxygen variability and mid-Pleistocene global changes. Paleobiology 45, 85–97. https://doi.org/10.1017/pab.2018.37.

Huang, Y., Tong, J., Tian, L., Song, H., Chu, D., Miao, X., Song, T., 2023. Temporal shell-size variations of bivalves in south China from the late Permian to the early middle Triassic. Palaeogeogr. Palaeoclimatol. Palaeoecol. 609, 111307 https://doi.org/10.1016/j.palaeo.2022.111307.

IPCC, 2021. In: Masson-Delmotte, V., Zhai, P., Pirani, A., Connors, S.L., Pean, C., Berger, S., Caud, N., Chen, Y., Goldfarb, L., Gomis, M.I., Huang, M., Leitzell, K., Lonnoy, E., Matthews, J.B.R., Maycock, T.K., Waterfield, T., Yelekci, O., Yu, R., Zhoo, B. (Eds.), Climate Change 2021: the Physical Science Basis. Contribution of Working Group I to the Sixth Assessment Report of the Intergovernmental Panel on Climate Change. Cambridge University Press.

IPCC, 2019. Special Report on the Ocean and Cryosphere in a Changing Climate, Working Group II. Technical Support Unit. Intergovernmental Panel on Climate Change.

Karlson, A.M.L., Pilditch, C.A., Probert, P.K., Leduc, D., Savage, C., 2021. Large infaunal bivalves determine community Uptake of Macroalgal Detritus and food web Pathways. Ecosystems 24, 384–402. https://doi.org/10.1007/s10021-020-00524-5.

Konijnendijk, T.Y.M., Ziegler, M., Lourens, L.J., 2015. On the timing and forcing mechanisms of late Pleistocene glacial terminations: insights from a new high-resolution benthic stable oxygen isotope record of the eastern Mediterranean. Quat. Sci. Rev. 129, 308–320. https://doi.org/10.1016/j.quascirev.2015.10.005.

Kruft Welton, R.A., Hoppit, G., Schmidt, D.N., Witts, J.D., Moon, B.C., 2023. The Clam before the Storm: a Meta analysis showing the effect of combined climate change stressors on bivalves. EGUsphere 1–30. https://doi.org/10.5194/egusphere-2023-287.

Kruskal, W.H., Wallis, W.A., 1952. Use of Ranks in one-Criterion variance analysis. J. Am. Stat. Assoc. 47, 583–621. https://doi.org/10.1080/01621459.1952.10483441.

La Perna, R., 2007. Taxonomy of the family Neilonellidae (Bivalvia, Protobranchia): Miocene and plio-Pleistocene species of Pseudoneilonella Laghi, 1986 from Italy. Veliger 49, 196–208.

La Perna, R., 2003. The Quaternary deep-sea protobranch fauna from the Mediterranean: composition, depth-related distribution and changes. Bolletino Malacol. Roma 39, 17–34.

Lin, C.-H., Wei, C.-L., Ho, S.L., Lo, L., 2023. Ocean temperature drove changes in the mesopelagic fish community at the edge of the Pacific Warm Pool over the past 460,000 years. Sci. Adv. 9, eadf0656 https://doi.org/10.1126/sciadv.adf0656.

Lisiecki, L.E., Raymo, M.E., 2005. Plio–Pleistocene climate evolution: trends and transitions in glacial cycle dynamics. Quat. Sci. Rev. 26, 56–69. https://doi.org/10.1016/j.quascirev.2006.09.005.

Lotze, H.K., Tittensor, D.P., Bryndum-Buchholz, A., Eddy, T.D., Cheung, W.W.L., Galbraith, E.D., Barange, M., Barrier, N., Bianchi, D., Blanchard, J.L., Bopp, L., Büchner, M., Bulman, C.M., Carozza, D.A., Christensen, V., Coll, M., Dunne, J.P., Fulton, E.A., Jennings, S., Jones, M.C., Mackinson, S., Maury, O., Niiranen, S., Oliveros-Ramos, R., Roy, T., Fernandes, J.A., Schewe, J., Shin, Y.-J., Silva, T.A.M., Steenbeek, J., Stock, C.A., Verley, P., Volkholz, J., Walker, N.D., Worm, B., 2019. Global ensemble projections reveal trophic amplification of ocean biomass declines with climate change. Proc. Natl. Acad. Sci. 116, 12907–12912. https://doi.org/10.1073/pnas.1900194116.

Maiorano, P., Bertini, A., Capolongo, D., Eramo, G., Gallicchio, S., Girone, A., Pinto, D., Toti, F., Ventruti, G., Marino, M., 2016. Climate signatures through marine isotope stage 19 in the Montalbano Jonico section (southern Italy): a land–sea perspective. Palaeogeogr. Palaeoclimatol. Palaeoecol. 461, 341–361. https://doi.org/10.1016/j.palaeo.2016.08.029.

Maiorano, P., Herbert, T.D., Marino, M., Bassinot, F., Bazzicalupo, P., Bertini, A., Girone, A., Nomade, S., Ciaranfi, N., 2021. Paleoproductivity modes in central Mediterranean during MIS 20—MIS 18: calcareous plankton and alkenone variability. Paleoceanogr. Paleoclimatology 36, e2021PA004259. https://doi.org/10.1029/2021PA004259.

Marino, M., Bertini, A., Ciaranfi, N., Aiello, G., Barra, D., Gallicchio, S., Girone, A., La Perna, R., Lirer, F., Maiorano, P., Petrosino, P., Toti, F., 2015. Paleoenvironmental and climatostratigraphic insights for marine isotope stage 19 (Pleistocene) at the Montalbano Jonico succession, south Italy. Quat. Int., The Quaternary System and its formal subdivision 383, 104–115. https://doi.org/10.1016/j.quaint.2015.01.043.

Marino, M., Girone, A., Gallicchio, S., Herbert, T., Addante, M., Bazzicalupo, P., Quivelli, O., Bassinot, F., Bertini, A., Nomade, S., Ciaranfi, N., Maiorano, P., 2020a. Climate variability during MIS 20–18 as recorded by alkenone-SST and calcareous plankton in the Ionian Basin (central Mediterranean). Palaeogeogr. Palaeoclimatol. Palaeoecol. 560, 110027 https://doi.org/10.1016/j.palaeo.2020.110027.

Marino, M., Girone, A., Gallicchio, S., Herbert, T., Addante, M., Bazzicalupo, P., Quivelli, O., Bassinot, F., Bertini, A., Nomade, S., Ciaranfi, N., Maiorano, P., 2020b. Climate variability during MIS 20–18 as recorded by alkenone-SST and calcareous plankton in the Ionian Basin (central Mediterranean). Palaeogeogr. Palaeoclimatol. Palaeoecol. 560, 110027 https://doi.org/10.1016/j.palaeo.2020.110027.

Marino, M., Rodrigues, T., Quivelli, O., Girone, A., Maiorano, P., Bassinot, F., 2022. Paleoproductivity proxies and alkenone precursors in the western Mediterranean during the early-middle Pleistocene transition. Palaeogeogr. Palaeoclimatol. Palaeoecol. 601, 111104 https://doi.org/10.1016/j.palaeo.2022.111104.

Martin-Garcia, G.M., Alonso-Garcia, M., Sierro, F.J., Hodell, D.A., Flores, J.A., 2015. Severe cooling episodes at the onset of deglaciations on the Southwestern Iberian margin from MIS 21 to 13 (IODP site U1385). Glob. Planet. Change 135, 159–169. https://doi.org/10.1016/j.gloplacha.2015.11.001.

Martin-Garcia, G.M., Sierro, F.J., Flores, J.A., Abrantes, F., 2018. Change in the North Atlantic circulation associated with the mid-Pleistocene transition. Clim. Past 14, 1639–1651. https://doi.org/10.5194/cp-14-1639-2018.

McClain, C., Rex, M., 2001. The relationship between dissolved oxygen concentration and maximum size in deep-sea turrid gastropods: an application of quantile regression. Mar. Biol. 139, 681–685. https://doi.org/10.1007/s002270100617.

McClymont, E.L., Sosdian, S.M., Rosell-Melé, A., Rosenthal, Y., 2013. Pleistocene sea-surface temperature evolution: early cooling, delayed glacial intensification, and implications for the mid-Pleistocene climate transition. Earth Sci. Rev. 123, 173–193. https://doi.org/10.1016/j.earscirev.2013.04.006.

Meadows, C.A., Grebmeier, J.M., Kidwell, S.M., 2019. High-latitude benthic bivalve biomass and recent climate change: Testing the power of live-dead discordance in the Pacific Arctic. Deep sea Res. Part II top. Stud. Oceanogr., the distributed Biological Observatory: a change. Detection Array in the Pacific Arctic Region 162, 152–163. https://doi.org/10.1016/j.dsr2.2019.04.005.

Melo, C.S., Martín-González, E., da Silva, C.M., Galindo, I., González-Rodríguez, A., Baptista, L., Rebelo, A.C., Madeira, P., Voelker, A.H.L., Johnson, M.E., Arruda, S.A., Ávila, S.P., 2022. Range expansion of tropical shallow-water marine molluscs in the NE Atlantic during the last interglacial (MIS 5e): Causes, consequences and utility of ecostratigraphic indicators for the Macaronesian archipelagos. Quat. Sci. Rev. 278, 107377 https://doi.org/10.1016/j.quascirev.2022.107377.

Milker, Y., Weinkauf, M.F.G., Titschack, J., Freiwald, A., Krüger, S., Jorissen, F.J., Schmiedl, G., 2017. Testing the applicability of a benthic foraminiferal-based transfer function for the reconstruction of paleowater depth changes in Rhodes (Greece) during the early Pleistocene. PLoS One 12, e0188447. https://doi.org/10.1371/journal.pone.0188447.

Mukhopadhyay, A., Paul, S., Poddar, A., Chattopadhyay, D., Saha, R., Basak, R., Prasad, S., 2023. Body size evolution of the Late Cretaceous bivalves from Ariyalur, southern India. Cretac. Res. 149, 105570 https://doi.org/10.1016/j.cretres.2023.105570.

Naafs, B.D.A., Hefter, J., Ferretti, P., Stein, R., Haug, G.H., 2011. Sea surface temperatures did not control the first occurrence of Hudson Strait Heinrich Events during MIS 16. Paleoceanography 26. https://doi.org/10.1029/2011PA002135.

Nomade, S., Bassinot, F., Marino, M., Simon, Q., Dewilde, F., Maiorano, P., Isguder, G., Blamart, D., Girone, A., Scao, V., Pereira, A., Toti, F., Bertini, A., Combourieu-Nebout, N., Peral, M., Bourlès, D.L., Petrosino, P., Gallicchio, S., Ciaranfi, N., 2019. High-resolution foraminifer stable isotope record of MIS 19 at Montalbano Jonico, southern Italy: a window into Mediterranean climatic variability during a low-eccentricity interglacial. Quat. Sci. Rev. 205, 106–125. https://doi.org/10.1016/j.quascirev.2018.12.008.

Novack-Gottshall, P.M., 2008. Using Simple body-size Metrics to estimate fossil body volume: Empirical Validation using Diverse Paleozoic Invertebrates. Palaios 23, 163–173. https://doi.org/10.2110/palo.2007.p07-017r.

Ohlberger, J., 2013. Climate warming and ectotherm body size – from individual physiology to community ecology. Funct. Ecol. 27, 991–1001. https://doi.org/10.1111/1365-2435.12098.

PAGES, P.I.W.G. of, 2016. Interglacials of the last 800,000 years. Rev. Geophys. 54, 162–219. https://doi.org/10.1002/2015RG000482.

Palomares, M.L.D., Pauly, D., 2022. SeaLifeBase. World Wide Web electronic publication [WWW Document]. SeaLifeBase. URL. www.sealifebase.org.

Parmesan, C., Yohe, G., 2003. A globally coherent fingerprint of climate change impacts across natural systems. Nature 421, 37–42. https://doi.org/10.1038/nature01286.

Passos, F.D., Machado, F.M., Fantinatti, A., 2019. Shell morphology of a new Brazilian species of the family Kelliellidae, with a brief review of the genus Kelliella (Mollusca: Bivalvia). Mar. Biodivers. 49, 207–219. https://doi.org/10.1007/s12526-017-0782-4.

Payne, J.L., McClain, C.R., Boyer, A.G., Brown, J.H., Finnegan, S., Kowalewski, M., Krause, R.A., Lyons, S.K., McShea, D.W., Novack-Gottshall, P.M., Smith, F.A., Spaeth, P., Stempien, J.A., Wang, S.C., 2011. The evolutionary consequences of oxygenic photosynthesis: a body size perspective. Photosynth. Res. 107, 37–57. https://doi.org/10.1007/s11120-010-9593-1.

Pena, L.D., Goldstein, S.L., 2014. Thermohaline circulation crisis and impacts during the mid-Pleistocene transition. Science 345, 318–322. https://doi.org/10.1126/science.1249770.

Peral, M., Blamart, D., Bassinot, F., Daëron, M., Dewilde, F., Rebaubier, H., Nomade, S., Girone, A., Marino, M., Maiorano, P., Ciaranfi, N., 2020. Changes in temperature and oxygen isotopic composition of Mediterranean water during the Mid-Pleistocene transition in the Montalbano Jonico section (southern Italy) using the clumped-isotope thermometer. Palaeogeogr. Palaeoclimatol. Palaeoecol. 544, 109603 https://doi.org/10.1016/j.palaeo.2020.109603.

Piazza, V., Ullmann, C.V., Aberhan, M., 2020. Temperature-related body size change of marine benthic macroinvertebrates across the Early Toarcian Anoxic Event. Sci. Rep. 10, 4675. https://doi.org/10.1038/s41598-020-61393-5.

Powell, E.N., Stanton, R.J., 1985. Estimating biomass and energy flow of molluscs in peleo-communities. Paleontology.

Quillévéré, F., Cornée, J.-J., Moissette, P., López-Otálvaro, G.E., van Baak, C., Münch, P., Melinte-Dobrinescu, M.C., Krijgsman, W., 2016. Chronostratigraphy of uplifted Quaternary hemipelagic deposits from the Dodecanese island of Rhodes (Greece). Quat. Res. 86, 79–94. https://doi.org/10.1016/j.yqres.2016.05.002.

Quillévéré, F., Nouailhat, N., Joannin, S., Cornée, J.-J., Moissette, P., Lécuyer, C., Fourel, F., Agiadi, K., Koskeridou, E., Escarguel, G., 2019. An onshore bathyal record of tectonics and climate cycles at the onset of the Early-Middle Pleistocene Transition in the eastern Mediterranean. Quat. Sci. Rev. 209, 23–39. https://doi.org/10.1016/j.quascirev.2019.02.012.

Quivelli, O., Marino, M., Rodrigues, T., Girone, A., Maiorano, P., Abrantes, F., Salgueiro, E., Bassinot, F., 2020. Surface and deep water variability in the Western Mediterranean (ODP Site 975) during insolation cycle 74: high-resolution calcareous plankton and molecular biomarker signals. Palaeogeogr. Palaeoclimatol. Palaeoecol. 542, 109583 https://doi.org/10.1016/j.palaeo.2019.109583.

Quivelli, O., Marino, M., Rodrigues, T., Girone, A., Maiorano, P., Bertini, A., Niccolini, G., Trotta, S., Bassinot, F., 2021. Multiproxy record of suborbital-scale climate changes in the Algero-Balearic Basin during late MIS 20 - Termination IX. Quat. Sci. Rev. 260, 106916 https://doi.org/10.1016/j.quascirev.2021.106916.

R Core Team, 2019. R: A Language and Environment for Statistical Computing.

Regattieri, E., Giaccio, B., Mannella, G., Zanchetta, G., Nomade, S., Tognarelli, A., Perchiazzi, N., Vogel, H., Boschi, C., Drysdale, R.N., Wagner, B., Gemelli, M., Tzedakis, P., 2019. Frequency and dynamics of millennial-scale variability during marine isotope stage 19: insights from the Sulmona basin (central Italy). Quat. Sci. Rev. 214, 28–43. https://doi.org/10.1016/j.quascirev.2019.04.024.

Rhodes, M.C., Thayer, C.W., 1991. Mass extinctions: ecological selectivity and primary production. Geology 19, 877–880. https://doi.org/10.1130/0091-7613(1991)019<0877:MEESAP>2.3.CO;2.

Rodrigues, T., Alonso-García, M., Hodell, D.A., Rufino, M., Naughton, F., Grimalt, J.O., Voelker, A.H.L., Abrantes, F., 2017. A 1-Ma record of sea surface temperature and extreme cooling events in the North Atlantic: a perspective from the Iberian Margin. Quat. Sci. Rev. 172, 118–130. https://doi.org/10.1016/j.quascirev.2017.07.004.

Rohling, E.J., Foster, G.L., Grant, K.M., Marino, G., Roberts, A.P., Tamisiea, M.E., Williams, F., 2014. Sea-level and deep-sea-temperature variability over the past 5.3 million years. Nature 508, 477–482. https://doi.org/10.1038/nature13230.

Rohling, E.J., Marino, G., Grant, K.M., 2015. Mediterranean climate and oceanography, and the periodic development of anoxic events (sapropels). Earth Sci. Rev. 143, 62–97. https://doi.org/10.1016/j.earscirev.2015.01.008.

Rosenberg, G., 2009. Malacolog 4.1. 1: a Database of Western Atlantic Marine Mollusca [WWW database (version 4.1. 1)]. URL. http://www.malacolog.org/.

Rossi, V., Azzarone, M., Capraro, L., Faranda, C., Ferretti, P., Macrì, P., Scarponi, D., 2018. Dynamics of benthic marine communities across the Early-Middle Pleistocene boundary in the Mediterranean region (Valle di Manche, Southern Italy): biotic and stratigraphic implications. Palaeogeogr. Palaeoclimatol. Palaeoecol. 495, 127–138. https://doi.org/10.1016/j.palaeo.2017.12.042.

Roy, K., Jablonski, D., Valentine, J.W., 2001. Climate change, species range limits and body size in marine bivalves. Ecol. Lett. 4, 366–370. https://doi.org/10.1046/j.1461-0248.2001.00236.x.

Sánchez Goñi, M.F., Extier, T., Polanco-Martínez, J.M., Zorzi, C., Rodrigues, T., Bahr, A., 2023. Moist and warm conditions in Eurasia during the last glacial of the middle Pleistocene transition. Nat. Commun. 14, 2700. https://doi.org/10.1038/s41467-023-38337-4.

Scarponi, D., Nawrot, R., Azzarone, M., Pellegrini, C., Gamberi, F., Trincardi, F., Kowalewski, M., 2022. Resilient biotic response to long-term climate change in the Adriatic Sea. Glob. Change Biol. 28, 4041–4053. https://doi.org/10.1111/gcb.16168.

Seitz, R.D., Lipcius, R.N., 2001. Variation in top-down and bottom-up control of marine bivalves at differing spatial scales. ICES J. Mar. Sci. 58, 689–699. https://doi.org/10.1006/jmsc.2001.1054.

Sorensen, M., 1984. Growth and mortality in two Pleistocene bathyal micromorphic bivalves. Lethaia 17, 197–210.

Stevens, G.C., 1989. The Latitudinal gradient in geographical range: how so Many species Coexist in the Tropics. Am. Nat. 133, 240–256.

Tabanelli, C., 2008. Associazioni di paleocomunita batiali a molluschi bentonici nel Pliocene della Romagna. Quad. Studi E Not. Storia Nat. Della Romagna 26, 1–80.

Titschack, J., Joseph, N., Fietzke, J., Freiwald, A., Bromley, R.G., 2013. Record of a tectonically-controlled regression captured by changes in carbonate skeletal associations on a structured island shelf (mid-Pleistocene, Rhodes, Greece). Sediment. Geol. 283, 15–33. https://doi.org/10.1016/j.sedgeo.2012.11.001.

Twitchett, R.J., 2007. The Lilliput effect in the aftermath of the end-Permian extinction event. Palaeogeogr. Palaeoclimatol. Palaeoecol., The Permian-Triassic Boundary Crisis and Early Triassic Biotic Recovery 252, 132–144. https://doi.org/10.1016/j.palaeo.2006.11.038.

Tzedakis, P.C., 2010. The MIS 11-MIS 1 analogy, southern European vegetation, atmospheric methane and the "early anthropogenic hypothesis.". Clim. Past 6, 131–144. https://doi.org/10.5194/cp-6-131-2010.

Urra, J., Utrilla, O., Gofas, S., Valencia, V.A., Farias, C., González-García, E., López-González, N., Fernández-Salas, L.M., Rueda, J.L., 2023. Late Pleistocene boreal molluscs in the Gulf of Cadiz: past and current oceanographic implications. Quat. Sci. Rev. 313, 108196 https://doi.org/10.1016/j.quascirev.2023.108196.

Van Hinsbergen, D.J.J., Krijgsman, W., Langereis, C.G., Cornée, J.-J., Duermeijer, C.E., Van Vugt, N., 2007. Discrete plio-Pleistocene phases of tilting and counterclockwise rotation in the southeastern Aegean arc (Rhodos, Greece): early Pliocene formation of the south Aegean left-lateral strike-slip system. J. Geol. Soc. 164, 1133–1144. https://doi.org/10.1144/0016-76492006-061.

Verberk, W.C.E.P., Atkinson, D., Hoefnagel, K.N., Hirst, A.G., Horne, C.R., Siepel, H., 2021. Shrinking body sizes in response to warming: explanations for the temperature–size rule with special emphasis on the role of oxygen. Biol. Rev. 96, 247–268. https://doi.org/10.1111/brv.12653.

Walther, G.-R., Post, E., Convey, P., Menzel, A., Parmesan, C., Beebee, T.J.C., Fromentin, J.-M., Hoegh-Guldberg, O., Bairlein, F., 2002. Ecological responses to recent climate change. Nature 416, 389–395. https://doi.org/10.1038/416389a.

Watson, S.-A., Peck, L.S., Tyler, P.A., Southgate, P.C., Tan, K.S., Day, R.W., Morley, S.A., 2012. Marine invertebrate skeleton size varies with latitude, temperature and carbonate saturation: implications for global change and ocean acidification. Glob. Change Biol. 18, 3026–3038. https://doi.org/10.1111/j.1365-2486.2012.02755.x.

Yasuhara, M., Cronin, T.M., 2008. Climatic influences on deep-sea Ostracode (crustacea) Diversity for the last three million Years. Ecology 89, S53–S65. https://doi.org/10.1890/07-1021.1.